© 2017. Published by The Company of Biologists Ltd | Development (2017) 144, 4137-4147 doi:10.1242/dev.158485

RESEARCH ARTICLE

Regulation of mitosis-meiosis transition by the ubiquitin ligase β-TrCP in male germ cells

Tadashi Nakagawa[1], Teng Zhang[2], Ryo Kushi[1], Seiji Nakano[1], Takahiro Endo[1], Makiko Nakagawa[1], Noriko Yanagihara[1], David Zarkower[2,3] and Keiko Nakayama[1,*]

ABSTRACT

The mitosis-meiosis transition is essential for spermatogenesis. Specific and timely downregulation of the transcription factor DMRT1, and consequent induction of *Stra8* expression, is required for this process in mammals, but the molecular mechanism has remained unclear. Here, we show that β-TrCP, the substrate recognition component of an E3 ubiquitin ligase complex, targets DMRT1 for degradation and thereby controls the mitosis-meiosis transition in mouse male germ cells. Conditional inactivation of *β-TrCP2* in male germ cells of *β-TrCP1* knockout mice resulted in sterility due to a lack of mature sperm. The β-TrCP-deficient male germ cells did not enter meiosis, but instead underwent apoptosis. The induction of *Stra8* expression was also attenuated in association with the accumulation of DMRT1 at the *Stra8* promoter in β-TrCP-deficient testes. DMRT1 contains a consensus β-TrCP degron sequence that was found to bind β-TrCP. Overexpression of β-TrCP induced the ubiquitylation and degradation of DMRT1. Heterozygous deletion of *Dmrt1* in β-TrCP-deficient spermatogonia increased meiotic cells with a concomitant reduction of apoptosis. Collectively, our data indicate that β-TrCP regulates the transition from mitosis to meiosis in male germ cells by targeting DMRT1 for degradation.

KEY WORDS: Spermatogenesis, Mitosis, Meiosis, Ubiquitin-proteasome system, β-TrCP1 (BTRC), β-TrCP2 (Fbxw11), Ubiquitin ligase, Dmrt1

INTRODUCTION

Spermatogenesis is a highly regulated process by which diploid spermatogonial stem cells undergo mitotic expansion and then differentiate into spermatocytes that progress through meiosis to produce haploid spermatids, which in turn undergo elongation to give rise to spermatozoa (Jan et al., 2012). In male mouse embryos, pre-Sertoli cells maintain germ cells mitotically quiescent in G_0 phase of the cell cycle. During the first postnatal week of life, seminiferous tubules undergo remodeling and germ cells migrate to the basal lamina of the tubules, where a spermatogonial stem cell niche is formed and the germ cells develop into spermatogonial stem cells. The first wave of spermatogenesis takes place synchronously. In the adult, however, the spermatogenic cycle starts asynchronously, with the result that distinct stages of spermatid development are apparent in different tubules, allowing for the continuous production of functional sperm.

In mammals, retinoic acid (RA), the active derivative of vitamin A, contributes to the switch from undifferentiated spermatogonia to differentiating spermatogonia, as well as the transition from mitosis to meiosis of differentiating spermatogonia. In the latter case, RA promotes meiosis by activating RA receptor-dependent transcription of meiotic inducers, including *Stra8* (Bowles and Koopman, 2007). The expression of STRA8 is robustly induced in preleptotene spermatocytes entering meiosis (Oulad-Abdelghani et al., 1996; Vernet et al., 2006; Zhou et al., 2008). In *Stra8* mutant mice, most preleptotene spermatocytes fail to enter meiosis (Anderson et al., 2008; Mark et al., 2008), suggesting that STRA8 controls the switch from mitotic proliferation to meiosis in male germ cells. RA responsiveness in undifferentiated spermatogonia is regulated by Doublesex and Mab-3-related transcription factor 1 (DMRT1), which inhibits meiosis entry by blocking *Stra8* transcription (Raymond et al., 1998; Matson et al., 2010). Accordingly, DMRT1 was shown to be downregulated by an unknown mechanism before the onset of meiosis (Matson et al., 2010). DMRT1 is expressed in the testis throughout life and is required for both Sertoli cell differentiation and germ cell migration and proliferation, reinforcing the importance of its specific and timely disappearance in male germ cells for execution of the mitosis-meiosis transition.

The SCF (SKP1, CUL1 and F-box protein) complex is an E3 ubiquitin ligase that comprises the RING domain-containing protein ROC1, the scaffold proteins SKP1 and CUL1, and an interchangeable F-box protein responsible for substrate recognition. This complex contributes to the regulation of many cellular processes, including proliferation, differentiation and death by targeting its substrate proteins for degradation by the ubiquitin-proteasome system (Petroski and Deshaies, 2005). In this latter system, ubiquitin is first activated by an E1 ubiquitin-activating enzyme in an ATP-dependent manner and is then transferred to an E2 ubiquitin-conjugating enzyme before attachment to the target protein mediated by an E3 ubiquitin ligase. The E3 thus recognizes specific substrates and facilitates or directly catalyzes ubiquitin transfer to these proteins. In most instances, the formation of a polyubiquitin chain on a target protein marks it for degradation by the 26S proteasome (Hershko and Ciechanover, 1998).

β-Transducin repeat-containing protein (β-TrCP; Fbxw11) is the substrate recognition subunit of an SCF complex that mediates the ubiquitylation of various substrates (Fuchs et al., 2004; Frescas and Pagano, 2008). Mammals express two distinct paralogs of β-TrCP – β-TrCP1 and β-TrCP2 – that manifest similar biochemical properties (Suzuki et al., 1999; Tan et al., 1999). Male mice deficient in β-TrCP1 show moderate disruption of spermatogenesis and fertility without other signs of illness or gross tissue abnormalities (Guardavaccaro et al., 2003; Nakayama et al., 2003). Furthermore, combined β-TrCP1 knockout and β-TrCP2 knockdown throughout the body of adult mice was associated with a pronounced testicular phenotype that was

[1]Division of Cell Proliferation, ART, Tohoku University Graduate School of Medicine, Sendai, Miyagi 980-8575, Japan. [2]Department of Genetics, Cell Biology, and Development, and Developmental Biology Center, University of Minnesota, Minneapolis, MN 55455, USA. [3]Masonic Cancer Center, University of Minnesota, Minneapolis, MN 55455, USA.

*Author for correspondence (nakayak2@med.tohoku.ac.jp)

N.Y., 0000-0002-4840-2274; K.N., 0000-0003-0134-6401

Received 16 August 2017; Accepted 27 September 2017

Development (2017) 144, 4137-4147 doi:10.1242/dev.158485

characterized by impairment of spermatogenesis and attributed to accumulation of the β-TrCP substrate SNAIL (Kanarek et al., 2010). However, the widespread expression of β-TrCP1/2 in the testis, including that in both male germ cells and Sertoli cells, combined with the intimate interaction between these cell types, has made it difficult to elucidate the molecular mechanism by which β-TrCP regulates spermatogenesis.

We have now examined the role of β-TrCP in spermatogenesis by conditional gene targeting in mice. We found that β-TrCP functions as a critical regulator of the mitosis-meiosis transition in male germ cells by targeting DMRT1 for degradation.

RESULTS

Generation of *β-TrCP2* conditional knockout (CKO) mice

β-TrCP1$^{-/-}$ male mice have previously been found to manifest reduced fertility accompanied by testicular accumulation of spermatocytes in metaphase I of meiosis (Guardavaccaro et al., 2003). However, we did not observe this phenotype in *β-TrCP1*$^{-/-}$ males generated in our laboratory (Nakayama et al., 2003), suggesting that the effect of *β-TrCP1* deletion on fertility may be dependent on genetic background or gene-targeting strategy. Given that the two β-TrCP paralogs in mammals are thought to be functionally redundant (Frescas and Pagano, 2008), loss of both β-TrCP1 and β-TrCP2 might be expected to have a more profound effect on fertility. Consistent with this notion, whole-body knockdown of β-TrCP2 in adult male *β-TrCP1*$^{-/-}$ mice resulted in a loss of sperm associated with accumulation of the β-TrCP substrate SNAIL in the testis (Kanarek et al., 2010). These findings thus indicated that β-TrCP plays an essential role in spermatogenesis. However, given that the expression of both β-TrCP1 and β-TrCP2 was downregulated in all tissues of these mice, it has been difficult to identify the substrate (or substrates) of β-TrCP responsible for this phenotype, as well as the tissues or cells in which β-TrCP supports spermatogenesis.

To clarify this issue, we set out to generate *β-TrCP1/2* double-knockout (DKO) mice in a cell type-specific manner and to examine testicular function in these animals. To this end, we first generated mice in which exon 5 of *β-TrCP2* is flanked by loxP sequences (*β-TrCP2*^{F} allele) (Nakagawa et al., 2015a) and then induced deletion of the floxed gene by crossing the corresponding animals with *Stra8-Cre* transgenic mice, which express Cre recombinase specifically in spermatogonia from 3 days postpartum (dpp) (Sadate-Ngatchou et al., 2008) (Fig. 1A). Exon 5 of *β-TrCP2* encodes the F-box domain, which is required for binding of β-TrCP2 to the SKP1-CUL1 scaffold, and its deletion induces a frameshift that generates a premature stop codon. Genomic polymerase chain reaction (PCR) analysis confirmed that exon 5 of *β-TrCP2* was indeed substantially deleted from 8 dpp in the testis of *Stra8-Cre;β-TrCP2*$^{F/F}$ [*β-TrCP2* conditional knockout (CKO)] mice (Fig. 1B), whereas reverse transcription (RT) and quantitative PCR (qPCR) analysis showed that the testicular abundance of *β-TrCP2* mRNA was reduced at 6 to 10 dpp (Fig. 1C). Male *β-TrCP2* CKO mice were as fertile as control (*Stra8-Cre*) males (Table 1), indicating that loss of β-TrCP2 function alone did not affect spermatogenesis, likely as a result of functional compensation by β-TrCP1.

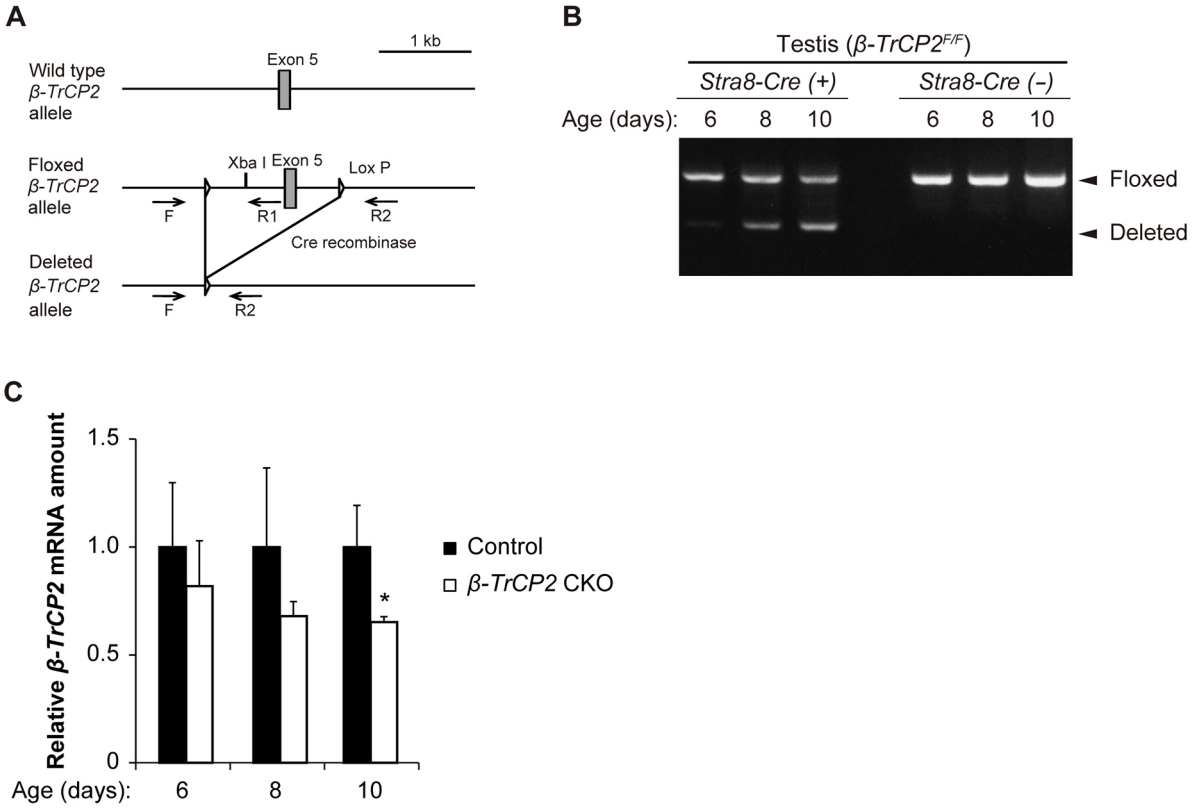

Fig. 1. Targeted disruption of the mouse *β-TrCP2* gene. (A) Schematic representation of wild-type, floxed and deleted alleles of the mouse *β-TrCP2* locus. LoxP sites are shown as triangles. Deletion of exon 5 by Cre recombinase results in a frameshift that generates a premature stop codon. The positions of PCR primers (F, R1, R2) for genotyping are indicated. (B) Genomic PCR analysis for the testis of *β-TrCP2* CKO or *β-TrCP2*$^{F/F}$ mice at the indicated ages. The remaining floxed band in *Stra8-Cre* animals is due to unrecombined alleles in somatic cells of the testis. (C) RT-qPCR analysis of *β-TrCP2* mRNA abundance in the testis of *β-TrCP2* CKO mice expressed relative to that for age-matched *β-TrCP2*$^{F/F}$ (control) mice. Data are mean±s.e.m. for three mice of each genotype. *P<0.05 versus corresponding control (two-way ANOVA followed by Tukey's post-hoc test).

Development (2017) 144, 4137-4147 doi:10.1242/dev.158485

Table 1. Fertility of male *β-TrCP* knockout mice

Genotype	Number of fertile mice/total	Litter size (mean±s.e.m.)*
Control	6/6	7.60±1.51
β-TrCP1 KO	6/6	5.85±1.78
β-TrCP2 CKO	6/6	7.22±1.64
β-TrCP1/2 DKO	0/6	0

*Resulting from 8-week-old male mice of the indicated genotype crossed with wild-type females

β-TrCP1/2 deletion in germ cells impairs fertility and spermatogenesis in adult male mice

To investigate the functional redundancy of the β-TrCP paralogs in male germ cells, we crossed *β-TrCP2*$^{F/F}$ mice with *β-TrCP1*$^{-/-}$ and *Stra8-Cre* mice to yield *Stra8-Cre;β-TrCP1*$^{-/-}$*;β-TrCP2*$^{F/F}$ (*β-TrCP1/2* DKO) male mice. Although neither *β-TrCP1* KO nor *β-TrCP2* CKO mice at 8 weeks of age manifested abnormalities, with both genotypes showing apparently normal fertility, male *β-TrCP1/2* DKO mice were completely sterile (Table 1) and their testes were significantly smaller than those of the single-knockout animals (Fig. 2A). Histological analysis revealed testicular atrophy with a greatly reduced number of sperm in *β-TrCP1/2* DKO epididymal (Fig. 2B) and seminiferous (Fig. 2C) tubules. These data thus indicated that β-TrCP in spermatogonia is essential for spermatogenesis and that β-TrCP paralogs are functionally redundant in male germ cells in this regard.

β-TrCP1/2 DKO mice manifest testicular vacuolization and apoptosis

To determine the developmental stage at which *β-TrCP1/2* deletion impairs spermatogenesis, we examined animals at various ages from 6 dpp, when a decrease in the expression of *β-TrCP2* in the testis of *β-TrCP2* CKO mice was first apparent (Fig. 1C). Testis weights of *β-TrCP1/2* DKO mice were significantly reduced compared with those in control mice beginning at 10 dpp (Fig. 3A). Although early meiotic events are first apparent in the testis of wild-type mice at 10 dpp (Bellve et al., 1977), some seminiferous tubules of *β-TrCP1/2* DKO mice contained germ cells with pyknotic nuclei, indicative of apoptosis, at this developmental stage (Fig. 3B). The pyknotic cells were observed at the center of tubules, not at the periphery where spermatogonia reside. At 14 dpp, meiotic germ cells that had migrated from the periphery to the center were evident in most tubules of control mice, whereas meiotic cells were essentially absent and the tubule lumen was largely empty in *β-TrCP1/2* DKO mice (Fig. 3B). The terminal deoxynucleotidyl transferase-mediated dUTP nick-end labeling (TUNEL) assay confirmed that apoptotic cells were located in the lumen of tubules and that the number of such cells was significantly increased in the *β-TrCP1/2* DKO mouse testis at 10 and 14 dpp (Fig. 3C). No significant increase in the number of apoptotic cells was apparent in the *β-TrCP1/2* DKO testis at 6 dpp (Fig. 3C). Together, these results suggested that loss of β-TrCP1/2 function in male germ cells leads to impairment of spermatogenesis by 10 dpp.

Male germ cells of *β-TrCP1/2* DKO mice do not enter meiosis

The developmental stage and location at which apoptotic cell death was observed in the *β-TrCP1/2* DKO mouse testis overlapped with those of early meiotic events in the testis of control mice, prompting us to examine whether germ cells of the mutant animals were eliminated before or after meiotic entry. Immunostaining revealed that the number of seminiferous tubules positive for SCP3, a marker of meiotic prophase, was markedly reduced in *β-TrCP1/2* DKO mice compared with control mice at 10 dpp (Fig. 4A,C). The paucity of

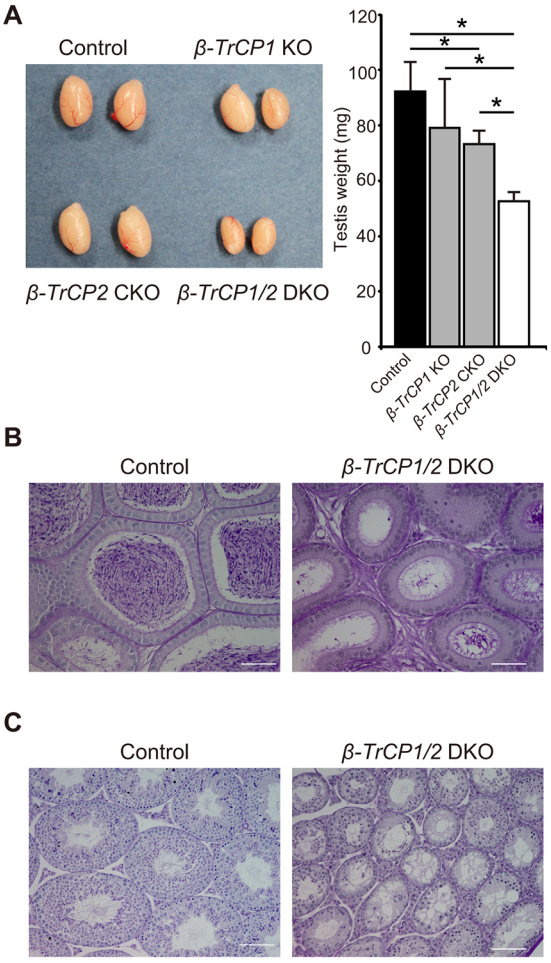

Fig. 2. Defective spermatogenesis in *β-TrCP1/2* DKO mouse testis. (A) Testis size and weight for *β-TrCP* knockout mice at 8 weeks of age. Quantitative data are mean±s.e.m. for six mice of each genotype. *P<0.05 versus age-matched control (one-way ANOVA followed by Tukey's post-hoc test). (B,C) Periodic acid-Schiff staining of epididymal (B) and seminiferous (C) tubules of 8-week-old control (*Stra8-Cre*) and *β-TrCP1/2* DKO mice. Scale bars: 100 µm.

staining for SCP3 in the mutant mice was more evident at 14 dpp (Fig. 4B,C), whereas staining for PLZF, a marker of undifferentiated spermatogonia, was similar in control and *β-TrCP1/2* DKO mice at both 10 and 14 dpp (Fig. 4). These results thus suggested that, whereas undifferentiated spermatogonia survive in *β-TrCP1/2* DKO mice, male germ cells do not enter meiotic prophase.

β-TrCP1/2 DKO male germ cells exhibit accumulation of DMRT1 with concomitant reduction of STRA8

Given that β-TrCP serves as the substrate binding component of an SCF ubiquitin ligase, its loss would be expected to reduce the ubiquitylation level of its substrates and (in most instances) to lead to their accumulation. To address the molecular mechanism for the meiotic defect in *β-TrCP1/2* DKO male germ cells, we first examined the abundance of various β-TrCP substrates implicated in spermatogenesis, as well as of mitotic (PLZF) and meiotic (DMC1) marker proteins. PLZF was detected from 6 to 10 dpp in the testis of control mice, and its level was not altered in that of *β-TrCP1/2* DKO mice (Fig. S1A). In contrast, induction of DMC1, a marker protein of meiotic prophase, was apparent at 10 dpp in the control testis, but this upregulation of DMC1 was greatly attenuated in the *β-TrCP1/2* DKO

Development (2017) 144, 4137-4147 doi:10.1242/dev.158485

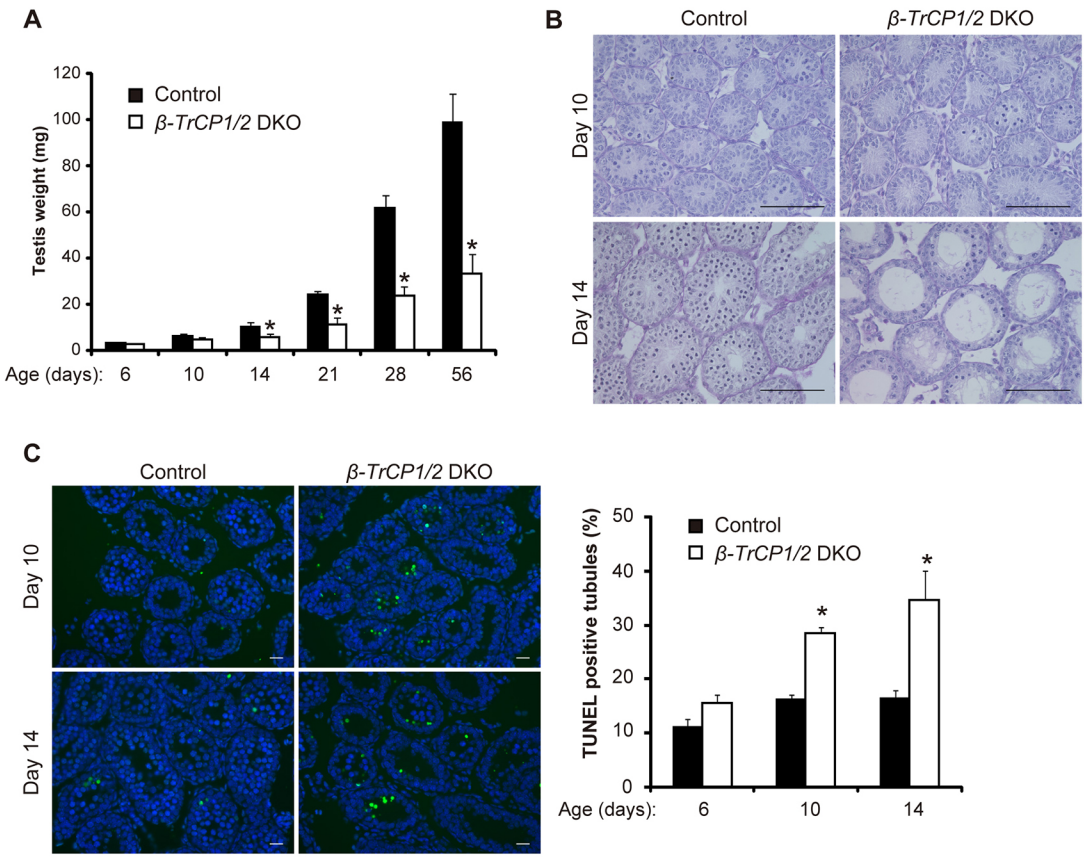

Fig. 3. Developmental defect and apoptosis in seminiferous tubules of *β-TrCP1/2* DKO mice. (A) Testis weight of control (*Stra8-Cre*) and *β-TrCP1/2* DKO mice at various ages. Data are mean±s.e.m. for four mice for each group. **P*<0.05 versus age-matched control (two-way ANOVA followed by Tukey's post-hoc test). (B) Periodic acid-Schiff staining of seminiferous tubules of control and *β-TrCP1/2* DKO mice at 10 and 14 dpp. Scale bars: 100 µm. (C) Left: TUNEL staining of seminiferous tubules in control and *β-TrCP1/2* DKO mice at 10 and 14 dpp. Scale bars: 10 µm. Right: The percentage of TUNEL-positive tubules was determined as mean±s.e.m. for three mice of each group. **P*<0.05 versus age-matched control (two-way ANOVA followed by Tukey's post-hoc test).

testis (Fig. S1A), providing further support for our finding that *β-TrCP1/2* is crucial for entry of male germ cells into meiotic prophase.

SNAIL and EMI1 have been implicated as targets of β-TrCP responsible for spermatogenic failure in *β-TrCP* mutant mice (Guardavaccaro et al., 2003; Kanarek et al., 2010). However, we found that neither of these proteins accumulated to a substantial extent in the testis of our *β-TrCP1/2* DKO mice (Fig. S1A). Bioinformatics analysis of meiosis-related proteins revealed that two such molecules – STRA8 and DMRT1 – contain a β-TrCP degron sequence (DSGXXS), to which β-TrCP has been found to bind (Hornbeck et al., 2012). Immunoblot analysis showed that the amount of DMRT1 was increased, whereas that of STRA8 was reduced in the *β-TrCP1/2* DKO testis compared with the control testis (Fig. 5A, Fig. S1A and S1B).

We have previously reported that DMRT1 is silenced at the mitosis-to-meiosis transition (Matson et al., 2010). We therefore used immunofluorescence to ask whether DMRT1 expression in double mutant testes is elevated specifically at this crucial regulatory step. We first examined spermatogonial markers (SOHLH1, SOHLH2 and DMRT6) and found that these were expressed in cells of appropriate morphology and organization, indicating that spermatogonial development is normal in the double mutant (data not shown). Next, we examined the mitosis/meiosis transition. In control testes, DMRT1 was expressed in Sertoli cells and spermatogonia, but not in SYCP3-positive preleptotene spermatocytes or prophase I spermatocytes (Fig. 5B, left panel). By contrast, in double mutant testes, many cells were present with morphology typical of preleptotene spermatocytes but expression of both DMRT1 and SYCP3 (Fig. 5B, middle and right panels) was severely defective in primary spermatocytes. We conclude that double mutant spermatogonia fail to properly downregulate DMRT1 at the onset of preleptonema and the ectopic DMRT1 likely interferes with initiation of meiotic prophase. DMRT1 regulates expression of *Stra8* in spermatogonia, likely by direct repression of *Stra8* transcription (Matson et al., 2010), and thus ectopic DMRT1 in double mutant testes would be expected to suppress the normal upregulation of STRA8 in preleptonema. In control testes, STRA8 was strongly expressed in preleptotene spermatocytes with characteristic speckled expression of SYCP3 and DAPI staining (Fig. 5C, left panels). Double mutant testes had a variable phenotype. In some tubules, preleptotene spermatocytes were present but lacked STRA8 (Fig. 5C, middle panels). These tubules lacked pachytene spermatocytes. Other tubules had some STRA8-positive preleptotene spermatocytes and pachytene spermatocytes with normally synapsed chromosomes but very few preleptotene cells had normal levels of STRA8 (Fig. 5C, right panels). β-TrCP1/2 DKO preleptotene cells exhibited DNA replication, marked by BrdU incorporation, similar to control cells (Fig. 5D) at 21 dpp when the second round of preleptotene cells replicate their DNA but Sertoli cells have already exited cell proliferation (Vergouwen et al., 1991). This indicates that loss of β-TrCP1/2 does not inhibit DNA replication of preleptotene cells, which takes place immediately before meiotic prophase.

Development (2017) 144, 4137-4147 doi:10.1242/dev.158485

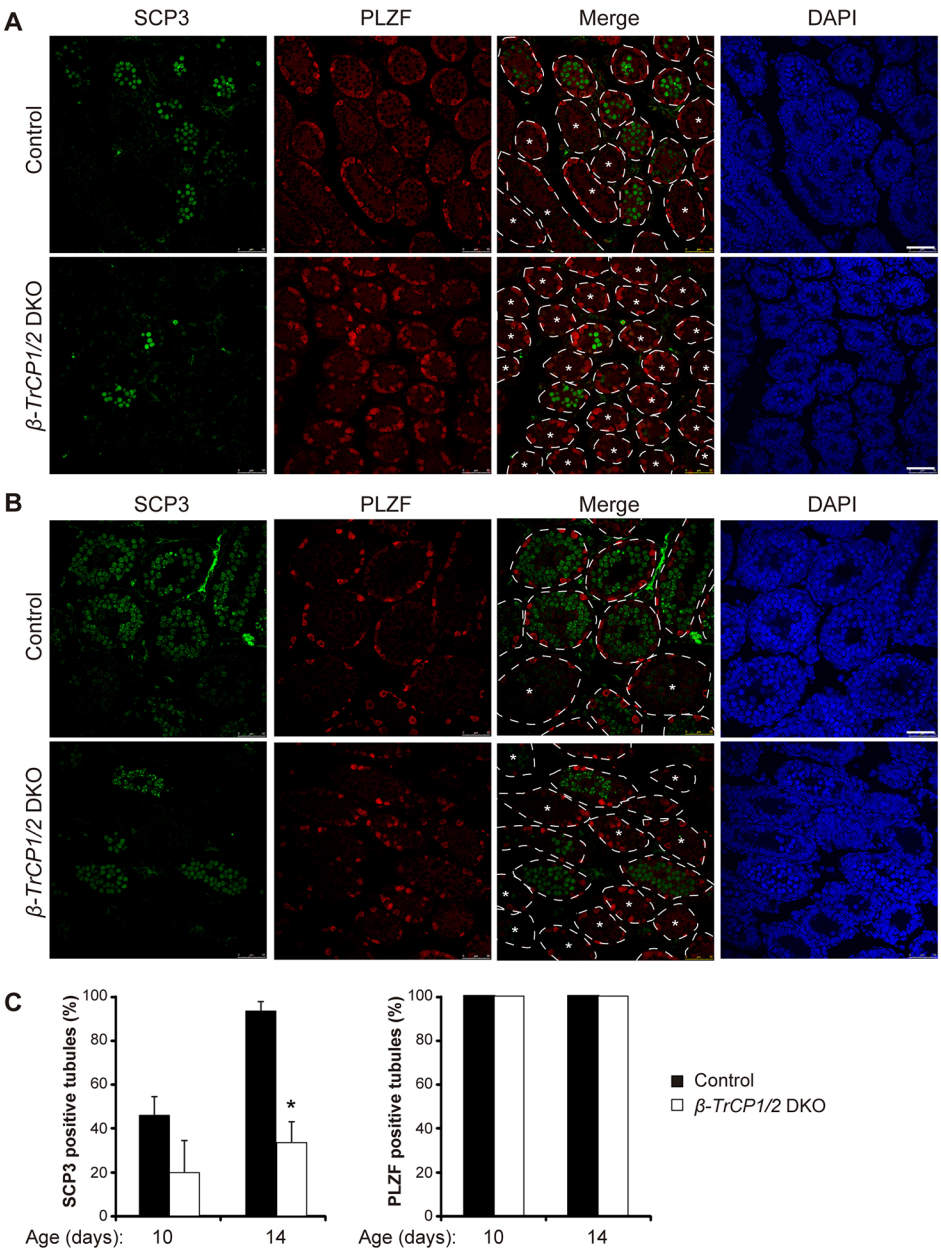

Fig. 4. Meiotic defect of male germ cells in *β-TrCP1/2* DKO mice.
(A,B) Immunohistofluorescence staining for SCP3 (green) and PLZF (red) in seminiferous tubules of control (*Stra8-Cre*) and *β-TrCP1/2* DKO mice at 10 (A) and 14 (B) dpp. The tubules are outlined in merged images on the basis of nuclear staining with 4′,6-diamidino-2-phenylindole (DAPI, blue). Seminiferous tubules lacking meiotic cells are indicated with an asterisk. Scale bars: 50 µm. (C) Percentage of seminiferous tubules containing SCP3$^+$ (left) or PLZF$^+$ (right) cells for control and *β-TrCP1/2* DKO mice at the indicated ages. Data are mean ±s.e.m. for three (for SCP3 staining) and two (PLZF staining) mice of each group. **P*<0.05 versus age-matched control (two-way ANOVA followed by Tukey's post-hoc test).

RT-qPCR analysis confirmed that *Stra8* expression was significantly decreased in the testis of *β-TrCP1/2* DKO mice compared with that of control mice at 8 dpp, whereas the abundance of *Dmrt1* mRNA did not differ between the two genotypes (Fig. 5E). Furthermore, chromatin immunoprecipitation (ChIP)-qPCR analysis showed that DMRT1 accumulated at the *Stra8* promoter in the *β-TrCP1/2* DKO testis (Fig. 5F), consistent with the notion that DMRT1 binds directly to the promoter region to repress *Stra8* expression (Matson et al., 2010). From these data, we conclude that ectopic DMRT1 expression in preleptonema is associated with reduced STRA8 expression and this likely contributes to the severe gametogenesis defects observed in the double mutant testes.

DMRT1 is a substrate of β-TrCP for ubiquitylation and degradation

The β-TrCP-binding motif (DSGXXS) of mouse DMRT1 is located at amino acids 329 to 334 (Fig. 6A), with phosphorylation of the two serine residues thought to be necessary for β-TrCP binding. Indeed, we found that DMRT1 bound to β-TrCP1 in testicular cells (Fig. 6B) and transfected 293T cells (Fig. 6C), as well as to β-TrCP2 in transfected 293T cells (Fig. 6D); however, an SA mutant of DMRT1, in which the serines at amino acid positions 330 and 334 have been replaced with alanine, did not. The ubiquitylation level of DMRT1 in transfected 293T cells was markedly increased by forced expression of either β-TrCP1 or β-TrCP2, whereas deletion of the F-box domain (ΔF) of either β-TrCP paralog abrogated this effect (Fig. 6E). In contrast, the SA mutant of DMRT1 was resistant to ubiquitylation even in cells overexpressing β-TrCP1 (Fig. 6F). Consistent with the degradation following ubiquitylation, overexpression of β-TrCP1 and β-TrCP2 markedly reduced the half-life of wild-type DMRT1 (Fig. 6G) but not the SA mutant of DMRT1 (Fig. S2A). Finally, Cre recombinase-mediated acute reduction of β-TrCP in mouse embryonic fibroblasts with reconstituted DMRT1 led to accumulation of steady-state levels of DMRT1 accompanied by the decrease in ubiquitylation level (Fig. S2B-D), supporting the notion that

Development (2017) 144, 4137-4147 doi:10.1242/dev.158485

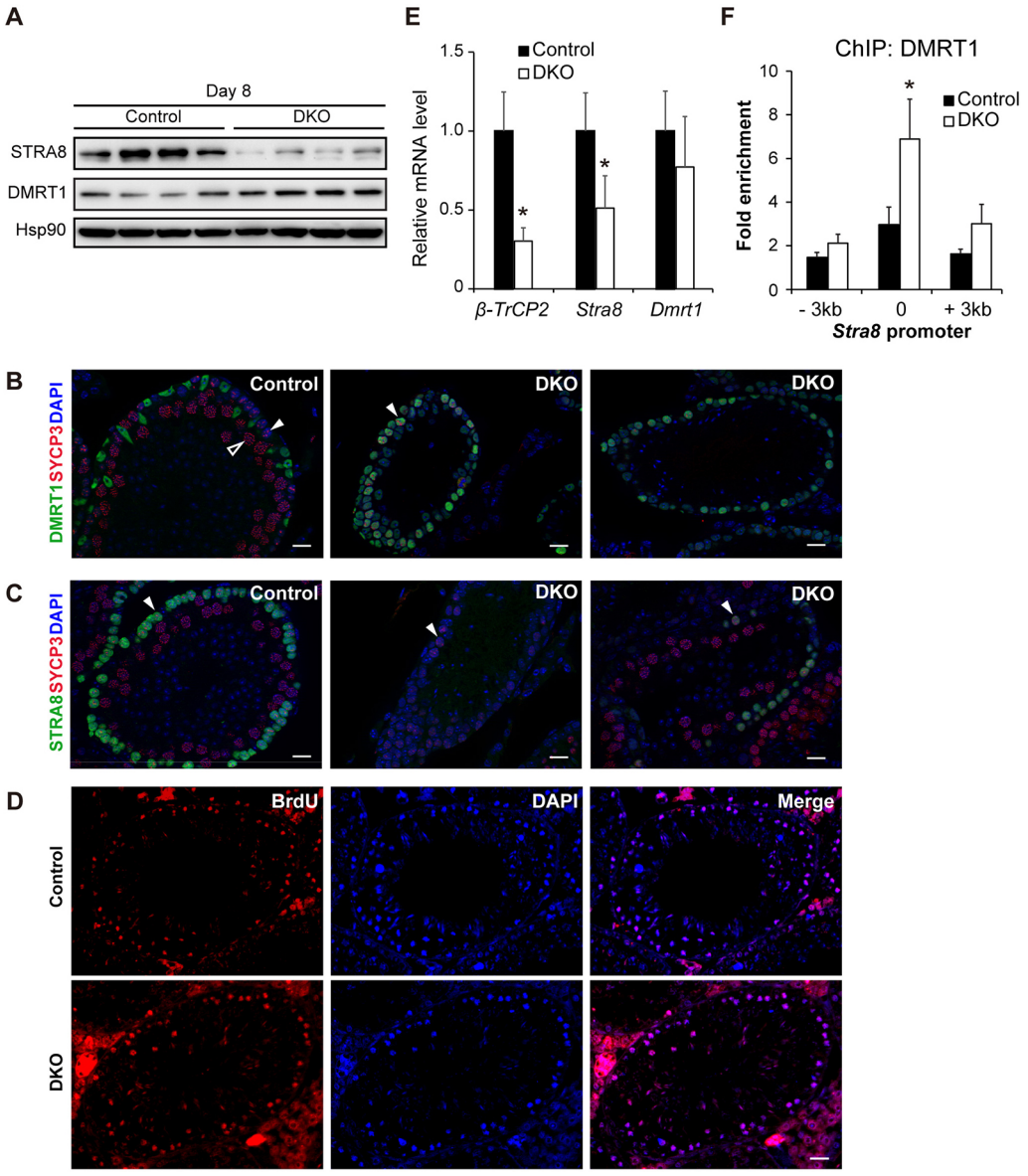

Fig. 5. Accumulation of DMRT1 and reduction of STRA8 in *β-TrCP1/2* DKO testes. (A) Immunoblot analysis of the indicated proteins in the testis of four control (*Stra8-Cre*, control) and four *β-TrCP1/2* DKO mice at 8 dpp. Hsp90 was examined as a loading control. (B) Immunofluorescent staining of sectioned adult seminiferous tubules for DMRT1 (green) and SYCP3 (red); DAPI staining of DNA is blue. In control testes (left panel), preleptotene spermatocytes (closed arrowhead) have speckled distribution of SYCP3 and lack DMRT1, whereas pachytene spermatocytes (open arrowhead) have filamentous SYCP3 localized to synaptonemal complexes. In double-mutant tubules (middle and right panels), preleptotene spermatocytes (closed arrowhead) ectopically express DMRT1 and pachytene spermatocytes are rare. (C) Immunofluorescent staining of sectioned seminiferous tubules STRA8 (green) and SYCP3 (red); DAPI staining of DNA is blue. In control testes (left panel), STRA8 is strongly expressed in preleptotene spermatocytes (closed arrowhead), whereas in double mutant testes (middle and right panels), STRA8 is absent or weakly expressed in these cells (closed arrowheads). Scale bars: 20 µm. (D) Analysis of BrdU incorporation (red) in sections of control and *β-TrCP1/2* DKO testes at 21 dpp. DAPI staining of DNA is blue. Scale bars: 20 µm. (E) RT-qPCR analysis of *β-TrCP2*, *Stra8* and *Dmrt1* mRNAs in the testis of control and *β-TrCP1/2* DKO mice at 8 dpp. Data are mean±s.e.m. for four mice of each genotype. **P*<0.05 versus control (unpaired Student's *t*-test). (F) ChIP-qPCR analysis of DMRT1 associated with the *Stra8* promoter in the testis of control and *β-TrCP1/2* DKO mice at 8 dpp. Regions (3 kb) upstream and downstream of the *Stra8* promoter were examined as negative controls. Data are mean±s.e.m. for three mice of each genotype. **P*<0.05 versus control (unpaired Student's *t*-test).

DMRT1 is targeted by β-TrCP for ubiquitylation and subsequent degradation.

Post-translational regulation of DMRT1 in germ cells

Our data indicated that downregulation of DMRT1 at the meiosis-to-mitosis transition is mediated by protein degradation, but not likely by transcriptional silencing. To confirm this, we used a Cre-inducible transgene to express DMRT1 and GFP in the adult spermatogonial lineage from a bicistronic mRNA (Lindeman et al., 2015). This transgene (*CAG-Stop-Dmrt1-Gfp*) is driven by a strong synthetic promoter followed by a transcriptional stop cassette that can be excised by Cre recombination to selectively activate transcription of the *Dmrt1*- and *Gfp*-coding sequences, and contains exogenous 5′ and 3′ untranslated regions (UTRs). We activated transgene transcription in undifferentiated spermatogonia by tamoxifen injection of adult mice carrying *CAG-Stop-Dmrt1-*

Development (2017) 144, 4137-4147 doi:10.1242/dev.158485

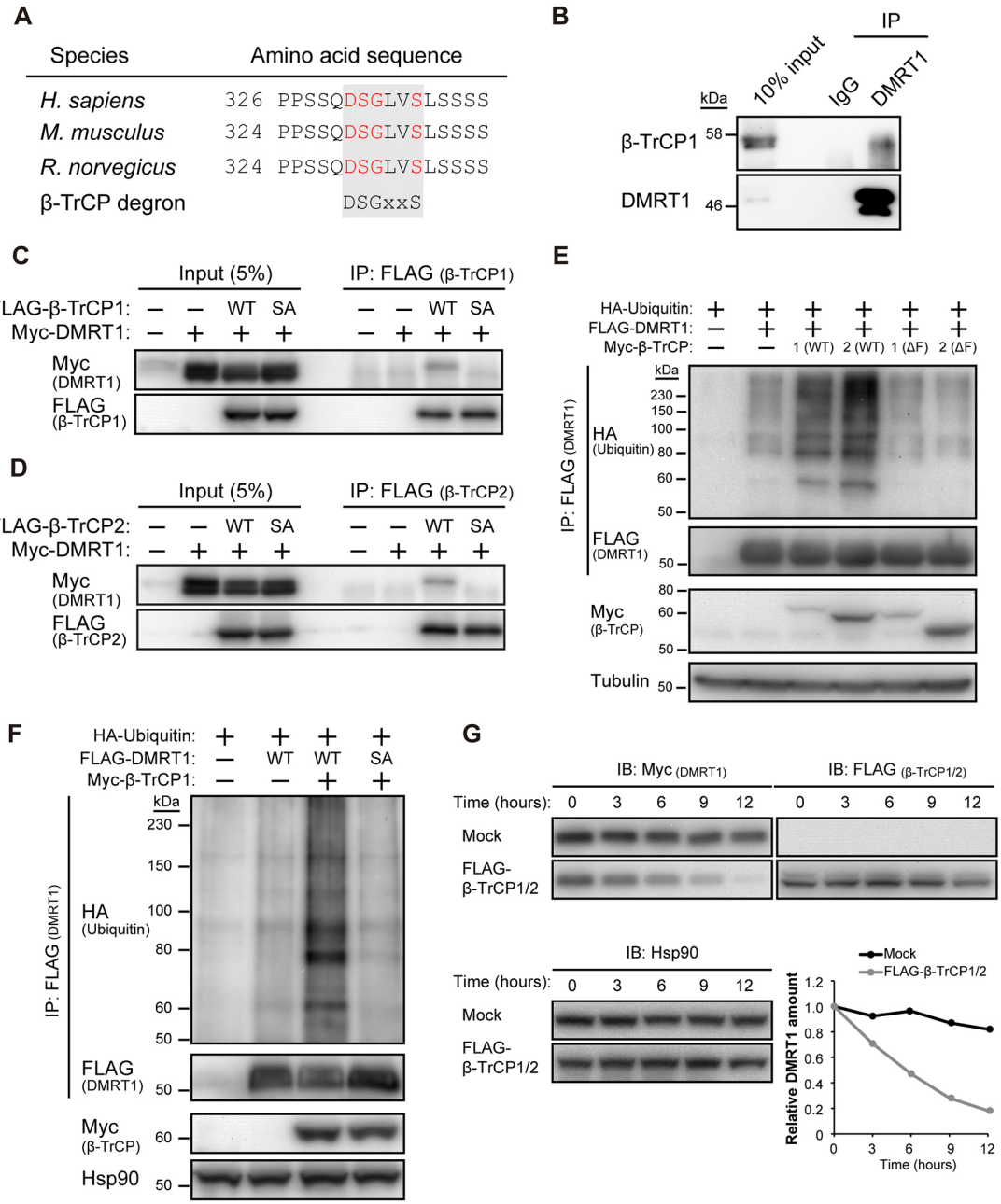

Fig. 6. β-TrCP1/2 bind to and ubiquitylate DMRT1 for degradation. (A) The amino acid sequences of DMRT1 orthologs. The β-TrCP degron is shaded, with the critical residues for association with β-TrCP indicated in red. (B) Immunoprecipitation analysis of the endogenous interaction of β-TrCP1 with DMRT1 in the control testis. Testis lysates were immunoprecipitated with antibodies to DMRT1 or control mouse IgG, and the immunoprecipitates (as well as 10% of the input lysates) were subjected to immunoblot analysis with antibodies to β-TrCP1 and to DMRT1. (C,D) Immunoprecipitation analysis of the interaction of β-TrCP1 (C) or β-TrCP2 (D) with DMRT1 in 293T cells transfected with expression vectors for FLAG epitope-tagged forms of β-TrCP1 or β-TrCP2, as well as for Myc epitope-tagged WT or SA mutant forms of DMRT1. Cell lysates were immunoprecipitated with antibodies to FLAG, and the immunoprecipitates (as well as 5% of the input cell lysates) were subjected to immunoblot analysis with antibodies to Myc and to FLAG. (E) *In vivo* ubiquitylation analysis of DMRT1. 293T cells transfected with vectors for hemagglutinin epitope (HA)-tagged ubiquitin, FLAG-tagged DMRT1 and Myc epitope-tagged WT or ΔF mutant forms of β-TrCP1 or β-TrCP2 were treated with the proteasome inhibitor MG132 for 5 h, lysed and subjected to immunoprecipitation with antibodies to FLAG under denaturing conditions followed by immunoblot analysis with antibodies to HA, to FLAG, to Myc and to tubulin (loading control). (F) *In vivo* ubiquitylation analysis of WT or SA mutant forms of DMRT1 with β-TrCP1 as in E. (G) Cycloheximide chase analysis of DMRT1 stability. 293T cells transfected with vectors for FLAG-tagged β-TrCP1 and β-TrCP2 (or the corresponding empty vector, mock), as well as for Myc epitope-tagged DMRT1 were incubated with cycloheximide for the indicated times, lysed and subjected to immunoblot analysis (IB) with the indicated antibodies. The band intensity for Myc-DMRT1 normalized by that of Hsp90 was quantified with Image J software.

Gfp and *Oct4-MerCreMer* (Greder et al., 2012) transgenes, and confirmed the co-expression of DMRT1 and GFP in spermatogonia by immunofluorescence (Fig. 7A-C). We next examined expression of DMRT1 and GFP in meiotic spermatocytes, identified based on morphology and SYCP3 expression (Fig. 7D-F). We asked whether exogenous transgene mRNA expression can cause ectopic expression of DMRT1 protein after the mitosis/meiosis transition. We found that activation of the transgene starting in spermatogonia

Development (2017) 144, 4137-4147 doi:10.1242/dev.158485

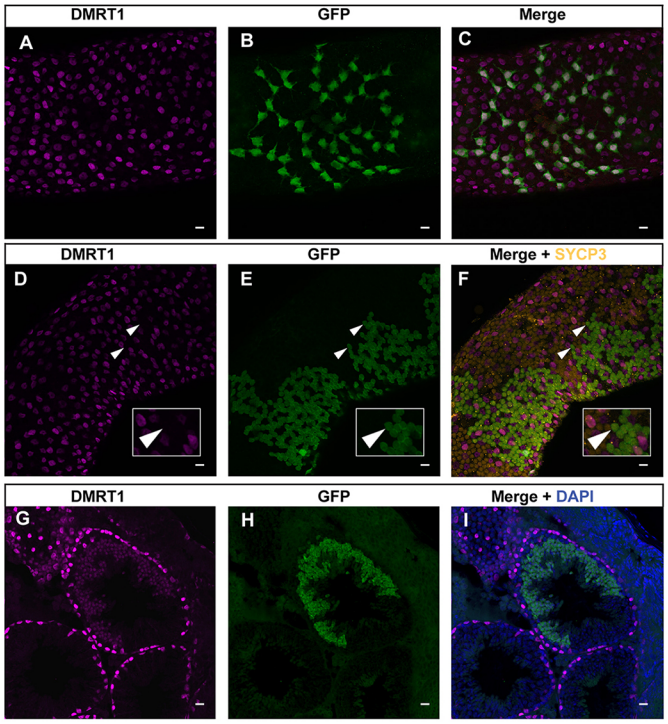

Fig. 7. Post-translational regulation of DMRT1 in germ cells. (A-C) Immunofluorescent staining of whole-mount seminiferous tubule for DMRT1 (magenta) and GFP (green). Strongly double-positive cells at surface of tubule are spermatogonia. (D-F) Immunofluorescent staining of whole-mount seminiferous tubule DMRT1 (magenta), GFP (green) and SYCP3 (orange). Large clones of GFP-positive cells below the tubule surface are spermatocytes and are SYCP3 positive and DMRT1 negative (arrowheads indicate examples of such cells). DMRT1-positive cells interspersed among SYCP3-positive spermatocytes are spermatogonia and Sertoli cells. Insets show the enlarged images of the cells indicated by arrowheads. (G-I) Immunofluorescent staining of seminiferous tubule section for DMRT1 (magenta) and GFP (green). Cells expressing GFP and DMRT1 are round spermatids. GFP immunofluorescence in whole-mount tubules is inefficient in spermatids and hence the strongly GFP-positive germ cells in E and F are primarily spermatocytes; GFP expression in spermatids is more readily apparent in cross-section, as in H and I, where the majority of strongly GFP-positive cells are round spermatid. Scale bars: 20 µm.

did result in GFP expression in large clones of spermatocytes, as expected (Fig. 7E); however, these cells did not express DMRT1 (arrowheads, Fig. 7D-F). As both proteins were translated from the same mRNA, we conclude that DMRT1 expression is likely silenced at the onset of meiosis by a mechanism involving regulated protein instability. In contrast to spermatocytes, transgenic DMRT1 was ectopically expressed in GFP-positive round spermatids (Fig. 7G-I), indicating that these cells lack the mechanism that destabilizes DMRT1.

Amelioration of spermatogenic defects in β-TrCP-deficient mice by heterozygous deletion of *Dmrt1*

To test our hypothesis that abnormal accumulation of DMRT1 is responsible for spermatogenic defects in β-TrCP mutant testes, we examined whether forced reduction of DMRT1 by heterozygous gene deletion prevented impairment of spermatogenesis. To this end, we first performed *in vitro* fertilization of oocytes obtained from *β-TrCP1*$^{-/-}$;*β-TrCP2*$^{F/F}$ mice with sperm from *Dmrt1*$^{F/F}$ mice (Raymond et al., 2000) to obtain *Dmrt1*$^{+/F}$;*β-TrCP1*$^{+/-}$;*β-TrCP2*$^{+/F}$ mice. As *Dmrt1* and *β-TrCP-1* are linked by the same chromosome (19, compared with *β-TrCP-2* on chromosome 11), we tried to obtain recombinants but were unable to obtain any. Therefore, we compared the testes of *Stra8-Cre;β-TrCP1*$^{+/-}$;*β-TrCP2*$^{F/F}$ (*β-TrCP1*$^{+/-}$;*β-TrCP2*$^{Δ/Δ}$) mice with those of *Stra8-Cre;Dmrt1*$^{+/F}$;*β-TrCP1*$^{+/-}$;*β-TrCP2*$^{F/F}$ (*Dmrt1*$^{+/Δ}$;*β-TrCP1*$^{+/-}$;*β-TrCP2*$^{Δ/Δ}$) and *Stra8-Cre;Dmrt1*$^{+/F}$ (*Dmrt1*$^{+/Δ}$) mice at 14 dpp when reduction of meiotic cells, increase of apoptosis and vacuolization of seminiferous tubules are notable in *β-TrCP1/2* DKO mice (Figs 3 and 4). As reported previously, heterozygous deletion of *Dmrt1* does not have any noticeable effects on spermatogenesis (Raymond et al., 2000) and thus *Dmrt1*$^{+/Δ}$ testis served as a control.

Compared with *Dmrt1*$^{+/Δ}$ mice, testis weight in *β-TrCP1*$^{+/-}$;*β-TrCP2*$^{Δ/Δ}$ mice was significantly reduced in association with vacuolization of seminiferous tubules, but *Dmrt1*$^{+/Δ}$;*β-TrCP1*$^{+/-}$;*β-TrCP2*$^{Δ/Δ}$ mice exhibited almost identical testis weight to control *Dmrt1*$^{+/Δ}$ mice with vacuolization ameliorated (Fig. 8A,B). Furthermore, increased apoptosis observed in *β-TrCP1*$^{+/-}$;*β-TrCP2*$^{Δ/Δ}$ mice was also significantly reduced in *Dmrt1*$^{+/Δ}$;*β-TrCP1*$^{+/-}$;*β-TrCP2*$^{Δ/Δ}$ mice (Fig. 8C and Fig. S3). Immunofluorescence analysis revealed the significant decrease in meiotic cells in *β-TrCP1*$^{+/-}$;*β-TrCP2*$^{Δ/Δ}$ seminiferous tubules, which was improved in *Dmrt1*$^{+/Δ}$;*β-TrCP1*$^{+/-}$;*β-TrCP2*$^{Δ/Δ}$ mice (Fig. 8D,E). Collectively, these data support the idea that abnormal accumulation of DMRT1 is a primary cause of spermatogenic defects in *β-TrCP* mutant testes.

DISCUSSION

Doublesex and Mab-3 (DM) domain-containing transcription factors mediate sexual differentiation following sex determination in both invertebrates and vertebrates (Matson and Zarkower, 2012). In male mice, DMRT1 is required for maturation of Sertoli cells, which support spermatogenesis, as well as for mitosis reinitiation and migration of germ cells (Raymond et al., 2000). DMRT1 must be downregulated after mitotic expansion for spermatogonia to enter meiosis (Matson et al., 2010), and the molecular mechanism of this downregulation has remained unknown. We have now demonstrated that this downregulation is mediated by post-transcriptional protein degradation and identified SCF$^{β\text{-TrCP}}$ as a critical ubiquitin ligase for this degradation in male germ cells immediately before meiotic entry. Although the importance of the ubiquitin-proteasome system in the late stages of spermatogenesis has been appreciated (Hou and Yang, 2013; Richburg et al., 2014), as far as we are aware, SCF$^{β\text{-TrCP}}$ is the first ubiquitin ligase shown to play a direct role in the mitosis-to-meiosis transition of germ cells in mammals.

How is SCF$^{β\text{-TrCP}}$-mediated degradation of DMRT1 restricted to the period immediately before meiosis? We consider two possibilities that are not mutually exclusive: (1) expression of β-TrCP1/2 is induced at this time; and (2) phosphorylation of the β-TrCP degron of DMRT1 occurs at this time. Given that recognition of substrates by F-box proteins is dependent on substrate phosphorylation and that we found that mutation of the putative phosphorylation sites in the β-TrCP degron of DMRT1 disrupted its binding to β-TrCP and consequent ubiquitylation in cells, the second scenario may be more likely. However, the kinase (or kinases) responsible for DMRT1 phosphorylation remains to be identified.

Both β-TrCP and DMRT1 are conserved from invertebrates to vertebrates, suggesting that regulation of DMRT1 by β-TrCP might also be conserved. However, this does not seem to be the case, given that neither the *Drosophila* DMRT1 ortholog Doublesex nor the *Caenorhabditis elegans* ortholog MAB-3 appears to contain a β-TrCP degron. The regulation of DMRT1 by β-TrCP might therefore have appeared after the evolutionary divergence of vertebrates from

Development (2017) 144, 4137-4147 doi:10.1242/dev.158485

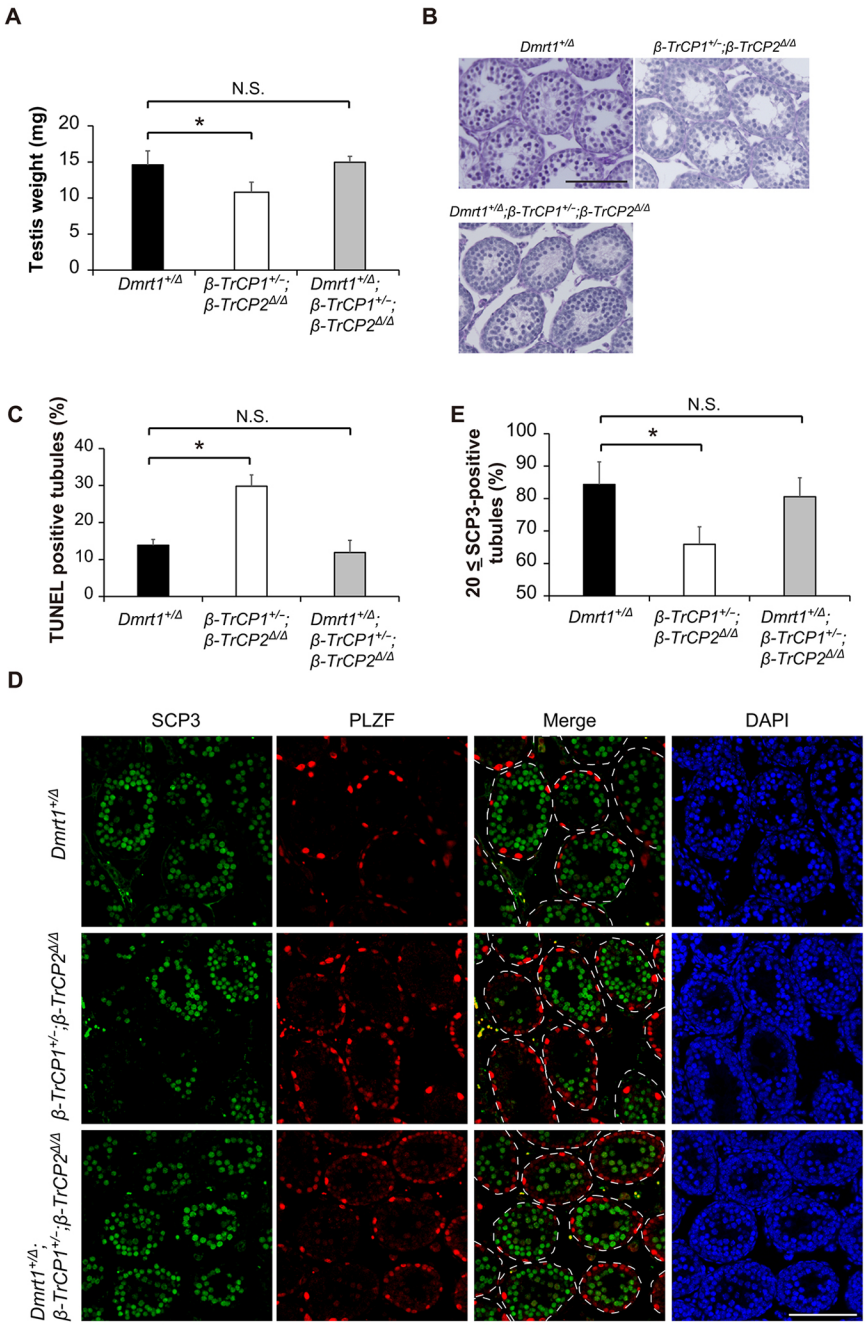

Fig. 8. Amelioration of spermatogenic defects in β-TrCP-deficient mice by heterozygous deletion of *Dmrt1*. (A) Testis weights of mice of indicated genotypes at 14 dpp. Data are mean±s.e.m. for three mice of each group. **P*<0.05 versus age-matched control (one-way ANOVA followed by Tukey's post-hoc test). N.S., not significant. (B) Periodic acid-Schiff staining of seminiferous tubules of mice of indicated genotypes at 14 dpp. Scale bar: 100 µm. (C) The percentage of TUNEL-positive tubules determined as the mean±s.e.m. for three mice of each group at 14 dpp. **P*<0.05 versus age-matched control (one-way ANOVA followed by Tukey's post-hoc test). N.S., not significant. See also Fig. S3. (D) Immunofluorescent staining for SCP3 (green) and PLZF (red) in seminiferous tubules of mice of indicated genotypes at 14 dpp. The tubules are outlined in merged images on the basis of nuclear staining DAPI (blue). Scale bar: 100 µm. (E) Percentage of seminiferous tubules containing 20 or more SCP3^{+} cells for mice of indicated genotypes at 14 dpp. Data are mean±s.e.m. for three mice of each group. **P*<0.05 versus age-matched control (one-way ANOVA followed by Tukey's post-hoc test). N.S., not significant.

invertebrates. Alignment of the amino acid sequences surrounding the β-TrCP degron of DMRT1 orthologs from fishes to mammals revealed that the critical sixth amino acid (serine) of the degron is not conserved in birds, in which it is replaced with cysteine (Fig. S4). The relevance of this difference remains unclear, but it is possible that the regulatory mechanism for meiotic entry of spermatogonia in birds differs from that in other vertebrates.

β-TrCP is one of the best-characterized F-box proteins, with β-TrCP1 and β-TrCP2 having been considered to be functionally redundant and indistinguishable. We found that *β-TrCP1/2* DKO male mice are sterile, whereas *β-TrCP1* KO and *β-TrCP2* CKO males are not. This finding is thus consistent with the notion of *β-TrCP* redundancy, at least in male germ cells.

Together, our results show that β-TrCP1/2 ubiquitylates DMRT1 and thereby targets it for degradation, with such degradation being necessary for the entry of spermatogonia into meiosis after their mitotic expansion. Our data are also consistent with the notion that phosphorylation of the β-TrCP degron of DMRT1 is the molecular trigger for the mitosis-to-meiosis switch. Identification of the kinase (or kinases) responsible for this phosphorylation should provide further insight into the molecular mechanisms underlying control of the proliferation and differentiation of spermatogonia.

MATERIALS AND METHODS

Generation of mutant mice and preparation of MEFs

β-TrCP-1$^{-/-}$ mice (Nakayama et al., 2003) and *β-TrCP2*$^{F/+}$ mice (Nakagawa et al., 2015a) were backcrossed to the C57BL/6 background for at least six generations. *Dmrt1*$^{F/F}$ mice (mainly C57BL/6 with a small amount of 129Sv and probably FVB) have been described previously (Raymond et al., 2000). *Stra8-Cre* mice on the FVB/NJ background [FVB/

Development (2017) 144, 4137-4147 doi:10.1242/dev.158485

N-Tg(Stra8-Cre) mice] were obtained from The Jackson Laboratory. *CAG-Stop-Dmrt1-Gfp* transgenic mice have been described previously (Lindeman et al., 2015). *Oct4-MerCreMer* knock-in mice were kindly provided by Dr Yoav Segal (University of Minnesota, MN, USA) (Greder et al., 2012). Mice were maintained in a specific pathogen-free facility at the Institute of Animal Experimentation (Tohoku University Graduate School of Medicine, Sendai, Japan) or at the University of Minnesota. They were provided with water and rodent chow *ad libitum* and treated according to The Standards for Humane Care and Use of Laboratory Animals of Tohoku University; to the Guidelines for Proper Conduct of Animal Experiments of the Ministry of Education, Culture, Sports, Science, and Technology of Japan; or to the University of Minnesota Animal Care and Use Committee. Primary mouse embryonic fibroblasts (MEFs) were obtained from 13.5 dpc embryos as described previously (Nakayama et al., 2003).

Isolation of RNA and RT-qPCR analysis

Testicular RNA was isolated and purified with the use of an SV Total RNA Isolation System (Promega) and was subjected to RT with the use of a PrimeScript RT reagent kit (Takara Bio) followed by real-time PCR analysis with a StepOnePlus Real-Time PCR System (Life Technologies) and Fast SYBR Green Master Mix (Life Technologies). Data were analyzed according to the $2^{-\Delta\Delta Ct}$ method and were normalized by the amount of Arbp mRNA as described previously (Hosogane et al., 2013). Sequences of PCR primers are provided in Table S1.

Histology, immunofluorescence analysis and BrdU incorporation

Testes were dissected and immediately fixed with 4% paraformaldehyde in phosphate-buffered saline (PBS) for 16 h at 4°C. The fixed tissue was dehydrated, embedded in paraffin wax and sectioned at 5 µm. After removal of paraffin wax, the sections were treated first with 0.5% periodic acid (Muto Pure Chemicals) for 10 min at 60°C and then with Schiff's reagent (Muto Pure Chemicals) for 20 min at room temperature. Nuclei were counterstained with Mayer's Hematoxylin (Muto Pure Chemicals). For immunostaining, sections were treated with boiling 20 mM sodium citrate buffer (pH 6.0) for 5 min, incubated with blocking solution (3% bovine serum albumin and 0.3% Triton X-100 in PBS) for 16 h at 4°C, and then exposed first to primary antibodies for 16 h at 4°C and then to Alexa Fluor 488- or Alexa Fluor 546-conjugated secondary antibodies for 1 h at room temperature. The sections were washed with PBS containing 0.1% Triton X-100, incubated with DAPI (1 µg/ml) for 10 min at room temperature, and then examined with a BZ9000 fluorescence microscope (Keyence), a DeltaVision fluorescence microscopy system (GE Healthcare) or a Zeiss Imager Z1 microscope with Apotome structured illumination using a Zeiss MRm camera. All the antibodies used in the present study are listed in Table S2, except for the STRA8 antibody used in Fig. 5C (Zhou et al., 2008), which was kindly provided by Dr. Michael D. Griswold (Washington State University, WA, USA). TUNEL staining was carried out using TUNEL Label Mix (Roche) and TUNEL Enzyme (Roche). BrdU incorporation assay was performed as described previously (Anderson et al., 2008).

Plasmid construction

The expression construct for HA ubiquitin has been described previously (Nakagawa et al., 2015b). The cDNAs encoding β-TrCP1 and β-TrCP2 were amplified from a cDNA library derived from mouse embryonic fibroblasts, and cloned into the pENTR vector (Life Technologies). The cDNA for DMRT1 was amplified from a library derived from mouse (C57BL/6) testis and also cloned into pENTR. The LR reaction was performed as described previously (Nakagawa et al., 2015b) to generate constructs for Myc epitope- or FLAG-tagged proteins. The SA mutant of DMRT1 and ΔF mutants of β-TrCP1 and β-TrCP2 were generated by PCR-based mutagenesis.

Cell culture and viral infection

MEFs and 293T cells (not recently authenticated) were maintained in Dulbecco's modified Eagle's medium supplemented with 10% fetal bovine serum, penicillin (50 U/ml), streptomycin (50 µg/ml), 2 mM L-glutamine, 1% MEM-non essential amino acids and 1% sodium pyruvate. Mycoplasma contamination tested monthly was negative. DMRT1 was reconstituted in *TrCP1*$^{-/-}$*;β-TrCP2*$^{F/F}$ MEFs by infection of retrovirus encoding DMRT1- and blasticidin-resistant genes, and infected cells were selected using 10 µg/ml blasticidin. Conditional deletion of the *β-TrCP2* gene in DMRT1-reconstituted MEFs was achieved by infection with a retrovirus containing Cre recombinase as described previously (Nakagawa et al., 2015a).

Immunoprecipitation and immunoblot analysis

For immunoprecipitation, 293T cells were washed with PBS and lysed for 10 min at 4°C in NP-40 lysis buffer [0.5% Nonidet P-40, 50 mM Tris-HCl (pH 7.5), 150 mM NaCl, 10% glycerol] and a protease inhibitor cocktail [10 µg/ml aprotinin (Sigma), 10 µg/ml leupeptin (Peptide institute) and 1 mM PMSF (Wako)]. The lysates were centrifuged at 20,000 ***g*** for 15 min at 4°C, and the resulting supernatants were incubated with Dynabeads Protein G (Life Technologies) conjugated with the antibodies to FLAG. The resulting immunoprecipitates were washed three times with PBS containing 0.1% Triton X-100 and 10% glycerol, and then subjected to immunoblot analysis.

For immunoblot assay, testicular extracts were prepared by homogenization of tissue in a solution containing 50 mM Tris-HCl (pH 7.5), 250 mM sucrose, 1 mM EDTA, a protease inhibitor cocktail and phosphatase inhibitor cocktail [0.4 mM sodium orthovanadate (Wako), 0.4 mM EDTA (Dojindo), 10 mM NaF (Wako) and 10 mM sodium pyrophosphate (Sigma)]. The homogenate was then mixed with an equal volume of 2× radioimmunoprecipitation assay (RIPA) buffer. Extracts of 293T cells were prepared with 1× RIPA buffer and were cleared of debris by centrifugation at 20,000 ***g*** for 15 min at 4°C. Band intensities were quantified using Image J software.

ChIP-qPCR analysis

ChIP-qPCR analysis was conducted as reported previously (Matson et al., 2010).

Ubiquitylation assay

The *in vivo* ubiquitylation assay was performed as described previously (Nakagawa et al., 2015b). In brief, 293T cells transfected with expression vectors for HA-ubiquitin, Myc epitope-tagged WT or ΔF mutant forms of β-TrCP1 or β-TrCP2, and FLAG-tagged WT or SA mutant forms of DMRT1 or MEFs reconstituted with DMRT1 were incubated with 10 µM MG132 for 5 h, lysed with NP-40 lysis buffer containing 0.1% SDS to disrupt noncovalent protein-protein interaction, and then subjected to immunoprecipitation with antibodies to FLAG followed by immunoblot analysis with the indicated antibodies.

Cycloheximide chase analysis

293T cells were incubated with cycloheximide (25 µg/ml) for the indicated times and then subjected to immunoblot analysis.

Bioinformatic protein sequence analysis

Mouse proteins with β-TrCP degron (DSGXXS) sequence were retrieved by 'SEQUENCE SEARCH' engine of PhosphoSitePlus (http://www.phosphosite.org/psrSearchAction.action) (Hornbeck et al., 2012), and reported functions of these proteins were obtained one by one based on literature.

Data reporting

Sample size was not predefined. The experiments were not randomized and the investigators were not blinded to allocation during experiments and outcome assessment.

Statistical analysis

Data are presented as mean±s.e.m. and were analyzed by the two-way analysis of variance (ANOVA) followed by Tukey's post-hoc tests or the unpaired Student's *t*-test as indicated in the figure legends. $P<0.05$ was considered statistically significant.

Acknowledgements

We thank the Biomedical Research Core of Tohoku University Graduate School of Medicine for technical support; M. Suzuki, H. Suda, Y. Nagasawa and T. Senga for technical assistance; T. Konishi for secretarial assistance; and other laboratory members for discussion.

Competing interests
The authors declare no competing or financial interests.

Author contributions
Conceptualization: T.N., N.Y., D.Z., K.N.; Methodology: T.N., T.Z., K.N.; Validation: T.N., T.Z., S.N., T.E., M.N.; Formal analysis: T.N., T.Z., R.K., S.N., T.E., M.N., N.Y.; Investigation: T.N., T.Z., R.K., S.N., T.E., M.N., N.Y., K.N.; Resources: D.Z.; Data curation: D.Z.; Writing - original draft: T.N., T.Z.; Writing - review & editing: D.Z., K.N.; Visualization: T.N., T.Z., K.N.; Supervision: D.Z., K.N.; Project administration: K.N.; Funding acquisition: T.N., D.Z., K.N.

Funding
This work was supported by funding from Japan Society for the Promotion of Science KAKENHI (19057001, 20370076, 21870006, 25891003, 26840059, 17K14955) and the US National Institutes of Health (NIH) (5 RO1 GM59152). Deposited in PMC for release after 12 months.

Supplementary information
Supplementary information available online at
http://dev.biologists.org/lookup/doi/10.1242/dev.158485.supplemental

References

Anderson, E. L., Baltus, A. E., Roepers-Gajadien, H. L., Hassold, T. J., de Rooij, D. G., van Pelt, A. M. M. and Page, D. C. (2008). Stra8 and its inducer, retinoic acid, regulate meiotic initiation in both spermatogenesis and oogenesis in mice. *Proc. Natl. Acad. Sci. USA* **105**, 14976-14980.

Bellve, A. R., Cavicchia, J. C., Millette, C. F., O'Brien, D. A., Bhatnagar, Y. M. and Dym, M. (1977). Spermatogenic cells of the prepuberal mouse. Isolation and morphological characterization. *J. Cell. Biol.* **74**, 68-85.

Bowles, J. and Koopman, P. (2007). Retinoic acid, meiosis and germ cell fate in mammals. *Development* **134**, 3401-3411.

Frescas, D. and Pagano, M. (2008). Deregulated proteolysis by the F-box proteins SKP2 and beta-TrCP: tipping the scales of cancer. *Nat. Rev. Cancer* **8**, 438-449.

Fuchs, S. Y., Spiegelman, V. S. and Kumar, K. G. (2004). The many faces of beta-TrCP E3 ubiquitin ligases: reflections in the magic mirror of cancer. *Oncogene* **23**, 2028-2036.

Greder, L. V., Gupta, S., Li, S., Abedin, M. J., Sajini, A., Segal, Y., Slack, J. M. W. and Dutton, J. R. (2012). Analysis of endogenous Oct4 activation during induced pluripotent stem cell reprogramming using an inducible Oct4 lineage label. *Stem Cells* **30**, 2596-2601.

Guardavaccaro, D., Kudo, Y., Boulaire, J., Barchi, M., Busino, L., Donzelli, M., Margottin-Goguet, F., Jackson, P. K., Yamasaki, L. and Pagano, M. (2003). Control of meiotic and mitotic progression by the F box protein beta-Trcp1 in vivo. *Dev. Cell* **4**, 799-812.

Hershko, A. and Ciechanover, A. (1998). The ubiquitin system. *Annu. Rev. Biochem.* **67**, 425-479.

Hornbeck, P. V., Kornhauser, J. M., Tkachev, S., Zhang, B., Skrzypek, E., Murray, B., Latham, V. and Sullivan, M. (2012). PhosphoSitePlus: a comprehensive resource for investigating the structure and function of experimentally determined post-translational modifications in man and mouse. *Nucleic Acids Res.* **40**, D261-D270.

Hosogane, M., Funayama, R., Nishida, Y., Nagashima, T. and Nakayama, K. (2013). Ras-induced changes in H3K27me3 occur after those in transcriptional activity. *PLoS Genet.* **9**, e1003698.

Hou, C.-C. and Yang, W.-X. (2013). New insights to the ubiquitin-proteasome pathway (UPP) mechanism during spermatogenesis. *Mol. Biol. Rep.* **40**, 3213-3230.

Jan, S. Z., Hamer, G., Repping, S., de Rooij, D. G., van Pelt, A. M. and Vormer, T. L. (2012). Molecular control of rodent spermatogenesis. *Biochim. Biophys. Acta* **1822**, 1838-1850.

Kanarek, N., Horwitz, E., Mayan, I., Leshets, M., Cojocaru, G., Davis, M., Tsuberi, B.-Z., Pikarsky, E., Pagano, M. and Ben-Neriah, Y. (2010). Spermatogenesis rescue in a mouse deficient for the ubiquitin ligase SCFβ-TrCP by single substrate depletion. *Genes Dev.* **24**, 470-477.

Lindeman, R. E., Gearhart, M. D., Minkina, A., Krentz, A. D., Bardwell, V. J. and Zarkower, D. (2015). Sexual cell-fate reprogramming in the ovary by DMRT1. *Curr. Biol.* **25**, 764-771.

Mark, M., Jacobs, H., Oulad-Abdelghani, M., Dennefeld, C., Feret, B., Vernet, N., Codreanu, C.-A., Chambon, P. and Ghyselinck, N. B. (2008). STRA8-deficient spermatocytes initiate, but fail to complete, meiosis and undergo premature chromosome condensation. *J. Cell Sci.* **121**, 3233-3242.

Matson, C. K. and Zarkower, D. (2012). Sex and the singular DM domain: insights into sexual regulation, evolution and plasticity. *Nat. Rev. Genet.* **13**, 163-174.

Matson, C. K., Murphy, M. W., Griswold, M. D., Yoshida, S., Bardwell, V. J. and Zarkower, D. (2010). The mammalian doublesex homolog DMRT1 is a transcriptional gatekeeper that controls the mitosis versus meiosis decision in male germ cells. *Dev. Cell* **19**, 612-624.

Nakagawa, T., Araki, T., Nakagawa, M., Hirao, A., Unno, M. and Nakayama, K. (2015a). S6 kinase- and β-TrCP2-dependent degradation of p19Arf is required for cell proliferation. *Mol. Cell Biol.* **35**, 3517-3527.

Nakagawa, T., Lv, L., Nakagawa, M., Yu, Y., Yu, C., D'Alessio, A. C., Nakayama, K., Fan, H.-Y., Chen, X. and Xiong, Y. (2015b). CRL4(VprBP) E3 ligase promotes monoubiquitylation and chromatin binding of TET dioxygenases. *Mol. Cell* **57**, 247-260.

Nakayama, K., Hatakeyama, S., Maruyama, S., Kikuchi, A., Onoe, K., Good, R. A. and Nakayama, K. I. (2003). Impaired degradation of inhibitory subunit of NF-kappa B (I kappa B) and beta-catenin as a result of targeted disruption of the beta-TrCP1 gene. *Proc. Natl. Acad. Sci. USA* **100**, 8752-8757.

Oulad-Abdelghani, M., Bouillet, P., Decimo, D., Gansmuller, A., Heyberger, S., Dolle, P., Bronner, S., Lutz, Y. and Chambon, P. (1996). Characterization of a premeiotic germ cell-specific cytoplasmic protein encoded by Stra8, a novel retinoic acid-responsive gene. *J. Cell Biol.* **135**, 469-477.

Petroski, M. D. and Deshaies, R. J. (2005). Function and regulation of cullin-RING ubiquitin ligases. *Nat. Rev. Mol. Cell. Biol.* **6**, 9-20.

Raymond, C. S., Shamu, C. E., Shen, M. M., Seifert, K. J., Hirsch, B., Hodgkin, J. and Zarkower, D. (1998). Evidence for evolutionary conservation of sex-determining genes. *Nature* **391**, 691-695.

Raymond, C. S., Murphy, M. W., O'Sullivan, M. G., Bardwell, V. J. and Zarkower, D. (2000). Dmrt1, a gene related to worm and fly sexual regulators, is required for mammalian testis differentiation. *Genes Dev.* **14**, 2587-2595.

Richburg, J. H., Myers, J. L. and Bratton, S. B. (2014). The role of E3 ligases in the ubiquitin-dependent regulation of spermatogenesis. *Semin. Cell. Dev. Biol.* **30**, 27-35.

Sadate-Ngatchou, P. I., Payne, C. J., Dearth, A. T. and Braun, R. E. (2008). Cre recombinase activity specific to postnatal, premeiotic male germ cells in transgenic mice. *Genesis* **46**, 738-742.

Suzuki, H., Chiba, T., Kobayashi, M., Takeuchi, M., Suzuki, T., Ichiyama, A., Ikenoue, T., Omata, M., Furuichi, K. and Tanaka, K. (1999). IkappaBalpha ubiquitination is catalyzed by an SCF-like complex containing Skp1, cullin-1, and two F-box/WD40-repeat proteins, betaTrCP1 and betaTrCP2. *Biochem. Biophys. Res. Commun.* **256**, 127-132.

Tan, P., Fuchs, S. Y., Chen, A., Wu, K., Gomez, C., Ronai, Z. and Pan, Z.-Q. (1999). Recruitment of a ROC1-CUL1 ubiquitin ligase by Skp1 and HOS to catalyze the ubiquitination of I kappa B alpha. *Mol. Cell* **3**, 527-533.

Vergouwen, R. P. F. A., Jacobs, S. G. P. M., Huiskamp, R., Davids, J. A. G. and de Rooij, D. G. (1991). Proliferative activity of gonocytes, Sertoli cells and interstitial cells during testicular development in mice. *J. Reprod. Fertil.* **93**, 233-243.

Vernet, N., Dennefeld, C., Guillou, F., Chambon, P., Ghyselinck, N. B. and Mark, M. (2006). Prepubertal testis development relies on retinoic acid but not rexinoid receptors in Sertoli cells. *EMBO J.* **25**, 5816-5825.

Zhou, Q., Nie, R., Li, Y., Friel, P., Mitchell, D., Hess, R. A., Small, C. and Griswold, M. D. (2008). Expression of stimulated by retinoic acid gene 8 (Stra8) in spermatogenic cells induced by retinoic acid: an in vivo study in vitamin A-sufficient postnatal murine testes. *Biol. Reprod.* **79**, 35-42.